Study on Shrinkage Characteristics of Heated Falling Liquid Films

Feng Zhang, Zhibing Zhang, and Jiao Geng
Dept. of Chemical Engineering, Nanjing University, Nanjing, 210093, China

DOI 10.1002/aic.10610
Published online August 9, 2005 in Wiley InterScience (www.interscience.wiley.com).

A liquid film flowing down along a heated solid surface may be substantially influenced by the Marangoni effect, which arises from the existence of a surface tension gradient that is induced by the variations of surface temperature in the transverse direction of the film, causing appreciable contraction of the film. In this work, the governing equations for laminar falling liquid films over a heated plate with constant surface temperature were solved and the surface temperature profile of the film was obtained. By considering the surface tension gradient and shrinkage characteristics in the brim of the heated film, a shrinkage model that gives the film interfacial area was derived based on the experimental infrared images. A comparison of the model with experimental data shows that the model can satisfactorily describe the flow characteristics of falling heated films. The model is expected to be useful for the design and operation of falling film equipments. © 2005 American Institute of Chemical Engineers *AIChE J,* 51: 2899–2907, 2005
Keywords: heat transfer, Marangoni effect, falling films, shrinkage model

Introduction

Falling films are usually used as the heat- and mass-transfer media in industrial equipment such as vertical condensers, film evaporators, and absorption towers.[1] In the processes of heated falling films, heat transfer occurs and interacts with film flow, leading to the variations of the liquid properties, especially viscosity and surface tension. Several researchers[2,3] indicated that the variations of liquid viscosity (thermoviscosity effects) would affect the film flow, whereas the nonuniformity of the surface tension at the liquid–gas interface, usually referred to as the *Marangoni effect*, could strongly influence the flow dynamics and thus the heat transfer.[4]

In recent years, interfacial instabilities of heated films such as the formation of surface waves, breaking of a stream into rivulets, and evaporation/termination of the liquid layer at a contact line, have been observed and theoretically analyzed.[5-10] Joo et al. studied the interfacial instability mechanism of heated falling films and derived a long-wave evolution equation to describe both the surface wave and the thermocapillary instability that were caused by either the gravity or the surface tension gradient. They concluded that the coupled temporal instabilities could create surface deformation and lead to an array of rivulets aligned with flow at moderate flow and heat-transfer rates.[10] In 1997, by completely solving the governing equations for the heated falling film, they further performed the three-dimensional simulation of the instabilities and rivulet formation. It was found that the spontaneous rupture and rivulet formation occurred even in a thin film under the combined influences of thermocapillary and surface-wave instabilities.[5] The Kabov research group[4,11-13] successfully performed experiments of heated falling films and developed a theoretical model to describe the influence of the Marangoni effect that was induced by the temperature and concentration gradients along the liquid–vapor interface. Very useful correlations for heat-transfer coefficient and film breakdown (including surface tension effect) were obtained, and the instabilities of a thin falling film, resulting from the Marangoni effect, were indicated to have a pattern of "regular horseshoe-like structures." This pattern of instable flow caused a decrease of the heat-transfer coefficient with an increase of the Reynolds number.[4] Skotheim et al.[6] also worked on the instability of the heated

Correspondence concerning this article should be addressed to Z. Zhang at segz@nju.edu.cn.

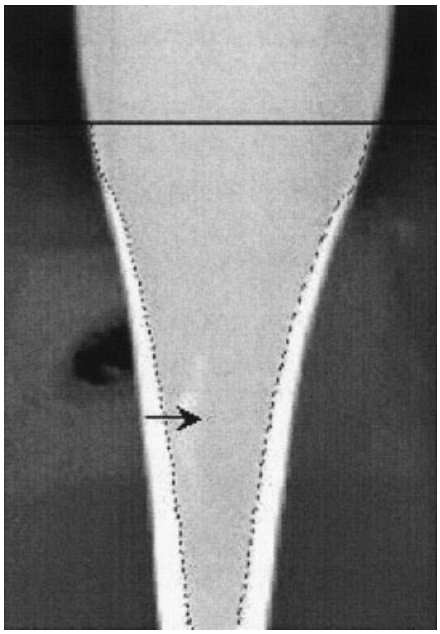

Figure 1. Shrinkage of the heated film.

falling films and showed that the surface tension gradients induced by the temperature difference, curvature pressure, gravity, and heat conduction could all influence the shape and stability of the steady flow profile. A model based on the long-wave evolution theory was proposed to describe the stationary curvature of the film and its stability, which were in good agreement with experimental data.

There are several studies on the dry patch forming in liquid films flowing over a heated surface. Some researchers[14-16] reported that the Marangoni effect induced by the surface tension gradient could substantially affect the dry patch formation. Zuber and Staub[14] observed the effects of the thermocapillary, the vapor thrust forces, as well as the forces arising from flow and surface wetting, on the dry patch. They thus presented a reasonable analysis for the prediction of the conditions that would permit a dry patch to form and remain stationary in a liquid film flowing over a heated surface. Shi and Zhang[16] analyzed the breakage of subcooled liquid film flowing down onto a heated plate with a simplified transverse deformation model and a dry patch model. The length of deformation area and critical film thickness were expressed as functions of surface tension coefficient and heat flux in their models, validating their analysis.

As a liquid film flows down over a heated surface, the variation of surface temperature occurs in both the streamwise and the transverse directions. The streamwise case arises from heat transfer and surface wave, whereas the transverse case arises from different flow rates in the brim of the film. Such temperature variations generate surface tension gradient and thermocapillary phenomena that are effective on the film flow. However, most of the work mentioned above took into account variations of surface temperature only in the streamwise direction. The variation in the transverse direction was usually ignored. In fact, the temperature gradient in the transverse direction is usually much higher than that in the streamwise direction (Figure 1) and might be more effective to heat transfer and film flow because the gravity-driven flow dominating in the streamwise direction is absent in the lateral direction.[5] This neglect may cause the correlative theory to stray largely from the experimental observation. In 2001, using water as the working fluid, our research group[17] performed experiments for the heat transfer of falling films (under no-evaporation condition) on a heated/cooled smooth stainless steel plate. It was found that the heated film was obviously contracted to form an inverse trapezoid, whereas the cooled film was expanded to form a right trapezoid. The width of the falling film decreased with increasing heating temperature, and vice versa. Actually, the shrinkage of heated film or expansion of cooled film was concluded to arise from the surface tension gradient in the transverse direction. For a heated film, temperature in the brim was higher than that in the center because of the slower flow and the sufficient heat transfer in the brim. This resulted in much smaller surface tension in the film margin than that in the center. The contraction of the film occurred under the effect of such surface tension gradient from brim to center of the film. In the case of the cooled film, the higher surface tension in the margin than that in the center leads to expansion of the film, which is completely opposite to the results obtained for the heated film. An infrared image is shown in Figure 1 to illustrate the surface temperature field of the heated liquid film that has initial uniform temperature. Different colors in the thermography represent different temperature magnitudes: the darker the color, the lower the temperature. The horizontal black solid line indicates the upper position of heater edge. It can be clearly seen that the heated film below the black solid line could be divided into two sections: the uniform central part, with an almost constant temperature, and the rim parts between dashed lines and boundaries of the film. The dashed lines are identified as temperature sidelines for the heated film. The transverse temperature curve of the heated film, located at about 0.05 m down from the upper edge of the heater, was recorded and shown in Figure 2 to have much higher temperature at the edges (the two peaks in the figure). Therefore, the evident surface tension gradient (shown by the arrow in Figure 1) attributed to the temperature gradient in the rim part apparently

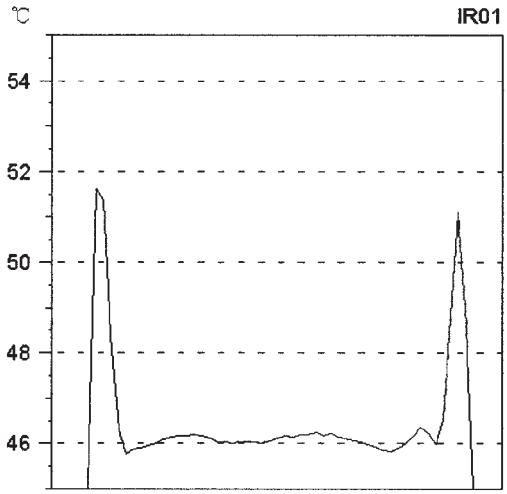

Figure 2. Transverse surface temperature of the heated film.

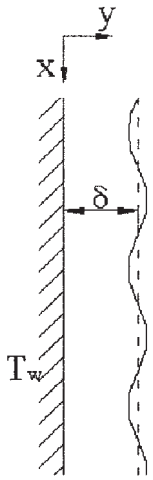

Figure 3. Heated falling film.

contracted the film, resulting in a substantial reduction of the interfacial transfer area.

Because of the absence of fundamental information concerning the hydrodynamics of the liquid film, mass- and heat-transfer analyses for industrial falling film equipment are still based on empirical methods in general. In a wetting wall column or a packed column the partial pressure driving force is determined by the conditions in the gas phase and the equilibrium concentrations of the solutes in the solvent. The remaining factors affecting the mass-transfer rate are the mass-transfer coefficient and the interfacial transfer area. The information that would permit separation of those two factors was not available, leading to the use of a combined coefficient, $K\alpha$, where K is the mass-transfer coefficient and α is the mass-transfer area per unit volume. Because K and α are both independent functions of the liquid conditions, use of a combined coefficient makes a rational analysis difficult.[18] As for heat-transfer equipment, the heat-transfer rate is determined by the interfacial area and the temperature difference between working fluid and heater. The interfacial area, usually regarded as the mechanical area of the heater, is overestimated because the heated liquid film could not completely cover the solid surface. The breakage of the liquid film and the dry patches may be frequently encountered in various common industrial heat- and mass-transfer equipment.

Therefore, for both heat- and mass-transfer processes, an understanding of the liquid film characteristics, especially the interfacial transfer area, is quite important. Based on the experimental infrared images done in this study, a governing equation for a heated film flowing down a vertical plate of constant wall temperature was presented to calculate the temperature profile of the falling film. Then, a shrinkage model will be further developed by taking into account the effect of the transverse temperature gradient on the film flow and Marangoni flow and be validated by designing and carrying out the experiments of heated falling films.

Theoretical

Model of heated liquid film flow

As shown in Figure 3, the surface of a thin liquid film flowing down a vertical plate under the gravity emerges with small waves. Compared with the average film thickness δ, the heights of these waves are negligibly small, so that the film surface can be regarded as smooth, as shown in Figure 4. Saouli[19] theoretically investigated heat transfer of a laminar falling film along an inclined plated with constant heat flux to successfully obtain the velocity and temperature profiles. In this work, a two-dimensional model for a fully developed laminar falling film over a vertical plate of constant wall temperature would be presented to obtain the film temperature profile in the central part.

Because the inertia term in the momentum equation is negligibly small compared to the body force term, the momentum equation in the direction x of gravity is simplified as

$$\mu \frac{\partial^2 u_x}{\partial y^2} + \rho g = 0 \tag{1}$$

where u_x is the velocity component in the x-direction; μ, ρ, and g represent the dynamic viscosity, liquid density, and gravitational acceleration, respectively. Because the temperature differences in both the x- and z-directions are very small compared to the temperature difference in the y-direction of the film, and flow rate in the z-direction is also negligible compared with u_x, heat transfers by convection in the z-direction and by conduction in the x- and z-directions are all neglected. Then, the governing energy equation can be expressed using the following equation

$$u_x \frac{\partial T(x, y)}{\partial x} = a \frac{\partial^2 T}{\partial y^2} \tag{2}$$

where $a = \lambda/\rho c_p$ represents for the thermal diffusivity.

The boundary conditions of no slip at the wall and no stress in the film surface are used for the momentum equation

$$y = 0 \qquad u_x = 0 \tag{3a}$$

$$y = \delta \qquad \frac{\partial u_x}{\partial y} = 0 \tag{3b}$$

The energy boundary conditions are as follows:

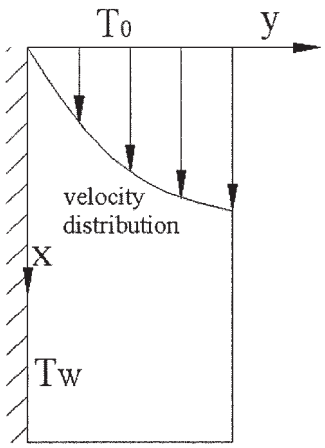

Figure 4. Physical model and coordinate system.

Initial Temperature of the Film

$$T(0, y) = T_0 \tag{4a}$$

Constant Temperature of the Plate Surface

$$T(x, 0) = T_w \tag{4b}$$

Adiabatic Film Surface

$$\frac{\partial T(x, \delta)}{\partial y} = 0 \tag{4c}$$

Integrating Eq. 1 leads to the expression of the velocity profile of the film

$$u_x = u_m\left[1 - \left(1 - \frac{y}{\delta}\right)^2\right] \tag{5}$$

where

$$u_m = \frac{1}{2}\left(\frac{\rho g}{\mu}\right)\delta^2 \tag{6}$$

The liquid mass flow rate per unit perimeter is

$$Q = \int_0^\delta \rho u_x dy \tag{7}$$

Substituting Eq. 5 in Eq. 7 generates the expression of the liquid film thickness

$$\delta = \left(\frac{3\mu Q}{\rho^2 g}\right)^{1/3} \tag{8}$$

Thus, by combining Eqs. 2 and 5, the energy equation can be rewritten as follows

$$u_m\left[1 - \left(1 - \frac{y}{\delta}\right)^2\right]\frac{\partial T(x, y)}{\partial x} = a\,\frac{\partial^2 T}{\partial y^2} \tag{9}$$

The following dimensionless variables were defined

$$Y = \frac{y}{\delta} \qquad X = \frac{ax}{u_m\delta^2} \qquad U(Y) = \frac{u(y)}{u_m}$$

$$\Theta(X, Y) = \frac{T(x, y) - T_0}{T_w - T_0} \tag{10}$$

By substituting Eq. 10 in Eqs. 9 and 4, neglecting the entrance effects, separating the variables, and integrating Eq. 9, we have the following expression

$$\Theta(X, Y) = \frac{12}{5}X + \frac{6}{5}(1 - Y)^2 - \frac{1}{5}(1 - Y)^4 \tag{11}$$

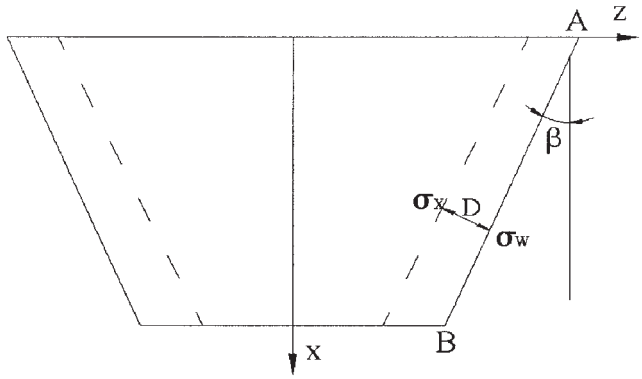

Figure 5. Shrinkage of a heated film.

Equation 11 is the working expression for the temperature profile of the liquid film.

Model for the shrinkage of heated film

Consideration of the surface tension gradient in the rim part and its effect on the heated falling film, suggests a model, as illustrated in Figure 5, for the expression of the film shrinkage in the initial section. The film is postulated to be symmetric to the central line (x-axis) of the film so that it is sufficient to analyze only one side of the film. In Figure 5, the z-direction is normal to the x–y plane as shown in Figure 4. For distinguishing the two parts of the film flow, a dashed line is drawn between the uniform central part and the rim part. The film in the uniform central part is assumed to be of constant thickness δ and constant flow rate Q, whereas the liquid within the rim part is regarded as flowing along the channel regulated by the dashed line and the contact line AB. Moreover, D stands for the width of the rim part and $(\sigma_x - \sigma_w\cos\theta)/D$ is the surface tension gradient in the rim. σ_x and σ_w represent the surface tension at the temperature of $T(x, \delta)$ and T_w, respectively. $T(x, \delta)$ represents the surface temperature of the liquid film in the uniform central part, and T_w the temperature of the plate surface. By neglecting the effect of gravity and inertia force that are negligibly small in the z-direction, the momentum equation in the z-direction of the rim becomes

$$\mu\,\frac{\partial^2 u_z}{\partial y^2} = 0 \tag{12}$$

The boundary conditions are as follows:

At the Wall

$$u_z = 0 \tag{12a}$$

At the Film Surface

$$\mu\,\frac{\partial u_z}{\partial y} = \frac{\partial \sigma}{\partial z}\cos\beta \tag{12b}$$

where u_z is the velocity component of the liquid flow in the z-direction and β is the angle of the tangent to the contact line with the x-direction.

By integrating Eq. 12 across the film using the above bound-

ary conditions and incorporating the Marangoni flow rate in the liquid layer as given by Kabov,[12] the velocity in the z-direction is derived to be

$$\mu \frac{u_z}{\delta} = \frac{(\sigma_x - \sigma_w \cos\theta)}{4D} \cos\beta \tag{13}$$

where θ is the contact angle along the contact line.

According to the illustration in Figure 5 we have $u_z/u_m = tg\beta$ and $\cos\beta = u_m/\sqrt{u_m^2 + u_z^2}$. Then Eq. 13 becomes

$$u_z = \frac{\delta(\sigma_x - \sigma_w \cos\theta)}{4\mu D} \frac{u_m}{\sqrt{u_m^2 + u_z^2}} \tag{14}$$

Defining

$$C = \frac{\delta}{4\mu D} (\sigma_x - \sigma_w \cos\theta) \tag{15}$$

and rearranging Eq. 14, lead to the following expression

$$u_z = \frac{\sqrt{2}}{2} u_m \left[\left(1 + \frac{4C^2}{u_m^2} \right)^{1/2} - 1 \right]^{1/2} \tag{16}$$

As the liquid film flowing down x distance on the heated plate, the shrinkage width ΔZ on one side of the film is

$$\Delta Z = \int_0^{x/u_m} u_z dt \tag{17}$$

where t represents the time and x/u_m is the time duration for the film flowing over x distance.

Substituting Eq. 16 into Eq. 17 produces the following expression

$$\Delta Z = \frac{\sqrt{2}}{2} \int_0^x \left[\left(1 + \frac{4C^2}{u_m^2} \right)^{1/2} - 1 \right]^{1/2} dx \tag{18}$$

It is assumed that the surface tension σ decreases linearly with the temperature: $\sigma = \sigma_0 + \gamma(T - T_0)$; then Eq. 15 becomes

$$C = \frac{\delta}{4\mu D} (\sigma_x - \sigma_w \cos\theta) = \frac{\delta}{4\mu D} [\sigma_w (1 - \cos\theta) + \gamma(T - T_w)] \tag{19}$$

where $T = T(x, \delta)$. When $y = \delta$, $Y = 1$, Eq. 11 is reduced to

$$\Theta(X, 1) = \frac{12}{5} X \tag{20}$$

By substituting Eq. 10 in Eq. 19, the following equation is obtained

$$\frac{T(x, \delta) - T_0}{T_\omega - T_0} = \frac{12}{5} \frac{ax}{u_m \delta^2} \tag{21}$$

The temperature of the surface without stress can thus be given as

$$T(x, \delta) = T_0 + \frac{12}{5} \Delta T \frac{ax}{u_m \delta^2} \tag{22}$$

where $\Delta T = T_\omega - T_0$.

Substituting Eq. 22 in Eq. 19 gives

$$C = \frac{\delta}{4\mu D} \left[\sigma_w (1 - \cos\theta) + \gamma \Delta T \left(\frac{12}{5} \frac{ax}{u_m \delta^2} - 1 \right) \right] = A_0 + Kx \tag{23}$$

where

$$A_0 = \frac{\delta}{4\mu D} (\sigma_0 - \sigma_w \cos\theta) \tag{24}$$

$$K = \frac{\delta \gamma \Delta T}{4\mu D} \frac{12}{5} \frac{a}{u_m \delta^2} = \frac{3\gamma \Delta T a}{5\mu D u_m \delta} \tag{25}$$

By combining Eq. 23 with Eq. 18 and then integrating, the shrinkage width of one side of the film can be finally expressed as

$$\Delta Z = \frac{\sqrt{2}}{6} \frac{u_m}{K} [(S_x^{3/2} - S_0^{3/2}) - 3(S_x^{1/2} - S_0^{1/2})] \qquad x \in [0, x_e] \tag{26}$$

where

$$S_x = \left[\left(\frac{2A_0 + 2Kx}{u_m} \right)^2 + 1 \right]^{1/2} + 1$$

$$S_0 = \left[\left(\frac{2A_0}{u_m} \right)^2 + 1 \right]^{1/2} + 1$$

$$\frac{A_0}{u_m} = \frac{\sigma_0}{\mu u_m} \frac{\delta}{4D} \left(1 - \frac{\sigma_w}{\sigma_0} \cos\theta \right)$$

$$\frac{K}{u_m} = \frac{3}{5} \frac{1}{D} \frac{\mathrm{Ma}_0}{\mathrm{Pe}^2}$$

$$x = x_e \qquad \text{when} \qquad T(x, \delta) = T_w$$

where x_e represents the length of the contracted film; $\mu u_m/\sigma_0$ is denoted as a dimensionless parameter called the Capillary number; $\mathrm{Ma}_0 = \gamma \Delta T \delta/\mu a$ stands for Marangoni number, which is a nondimensional measure of the surface tension gradient; and $\mathrm{Pe} = u_m \delta/\alpha$ is denoted as the Péclet number. Equation 26 provides a new way to numerically calculate the shrinkage

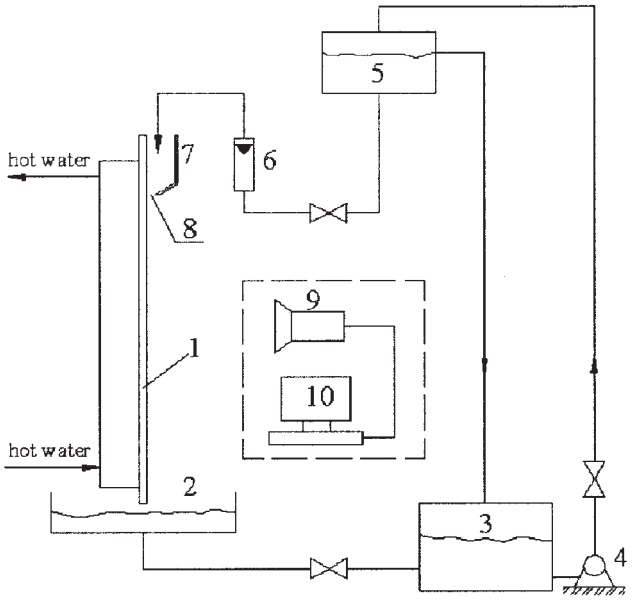

Figure 6. Experimental system.

Legend: 1: test section; 2: liquid collection vessel; 3: liquid storage tank; 4: pump; 5: upper tank; 6: rotameter; 7: fluid distributor; 8: liquid exit gap; 9: infrared camera; 10: computer.

width of a liquid film flowing down a heated vertical plate. It implies that the shrinkage width is affected by the flow rate, the physical properties of liquid, the temperature difference of ($T_w - T_0$), and the initial width of the liquid film (contained in the three nondimensional parameters $\mu u_m/\sigma_0$, Ma_0, and Pe). D, the width of the rim part, is also a very important parameter. The transverse temperature gradient and surface tension gradient are enhanced as D decreases, resulting in dramatic film contraction.

Experimental

Experimental setup

To determine the unknown variable D and to obtain the shrinkage width of the heated film, an experimental setup as shown in Figure 6 was designed. The test section [900 × 300 × 6 mm (length × width × thickness)] of the stainless steel plate was carefully polished. The experiment was expected to allow the liquid film to flow down at a scheduled flow rate over the vertical plate, being indirectly heated by hot water at a preset temperature. The surface temperature of the plate could be maintained by the hot water at a given temperature. The cool water source, used as the experiment media, was also maintained by a storage tank at a constant temperature. Distilled water in the storage tank was pumped to an upper tank and then flowed down to the test section at a scheduled flow rate. The flow rate ranging from 0.03 to 0.36 kg m^{-1} s^{-1} was measured with a rotameter. The liquid from the upper tank entered a fluid distributor installed in the upper position of the test section. The liquid exit gap could be adjusted manually to create liquid films of different thicknesses according to the needs of the experiments. The liquid flowing down the plate was collected by a vessel and recycled to the storage tank. Five Pt-100 thermal resistances were also installed to measure the temperature values of the film inlet and outlet, storage tank, upper tank, and the air near the film, respectively. The uncertainty of these temperature values was within ±0.1°C. The surface temperature and the shape of the film were determined by a highly sensitive infrared camera, Therma CAM ™ SC3000 (FLIR Systems, Inc., Portland, OR). Because the film edge was very thin, temperature at the edge of the film was regarded as the surface temperature of the wall, T_w.

The initial temperature of the falling water film was set and maintained at several constant values during the experiments (T_0 = 20–35°C). The temperature of plate surface T_w was controlled as the temperature of hot water ranging from 30 to 70°C. The physical characteristics of working fluid and basic experiment parameters are given in Table 1.

Characteristics of heated falling liquid films

The experiment shows that the flow of the heated falling liquid film is mainly affected by the temperature difference ($T_h - T_0$) and the film flow rate. As ($T_h - T_0$) increases, the liquid film apparently contracts and becomes very narrow. The reason is that the surface tension gradient in the transverse direction of the film is enhanced. The effect of the flow rate on the shrinkage of the heated film flow is quite complex. On one hand, a fast film flow rate is beneficial to the lateral expansion of the film. On the other hand, both film temperature and the rim width D decrease with an increase of flow rate, and the transverse surface temperature gradient correspondingly increases in the rim of the film. Therefore, the surface tension gradient is also increased, thus apparently causing the film to contract. For example, as shown in Figure 7, the heated film at a flow rate 0.03 kg m^{-1} s^{-1} is quite narrow, but then increases appreciably with liquid flow rate, increasing from 0.03 to 0.12 kg m^{-1} s^{-1}. However, when the flow rate is >0.12 kg m^{-1} s^{-1}, the film width starts to increase slowly. Interestingly, the quick liquid contraction is found only near the entrance, but the width tends to keep constant to the end after the liquid flows beyond a certain distance. This phenomenon may imply that the effect of viscous force and the lateral expansion effect of the liquid flow are finally balanced with Marangoni effect in the transverse direction of the film.

Table 1. Physical Characteristics of Working Fluid and Operation Parameters

Physical Characteristics	Operation Parameters
Working fluid: distilled water	Flow rate, Q: 0.03–0.36 kg m^{-1} s^{-1}
Initial temperature, T_0: 20–30°C	Temperature of hot water, T_h: 30–70°C
Density, ρ: 995.3–998.5 kg/m^3	Reynolds number, Re = $4Q/\mu$: 137–2024
Viscosity, μ: 7.16–9.90 × 10^{-4} Pa · s	Prandtl number, Pr = $C_P\mu/\lambda$: 4.79–6.91
Surface tension, σ: 70.6–72.9 dyn/cm	
Heat conductivity, λ: 0.5997–0.6241 W m^{-1} k^{-1}	

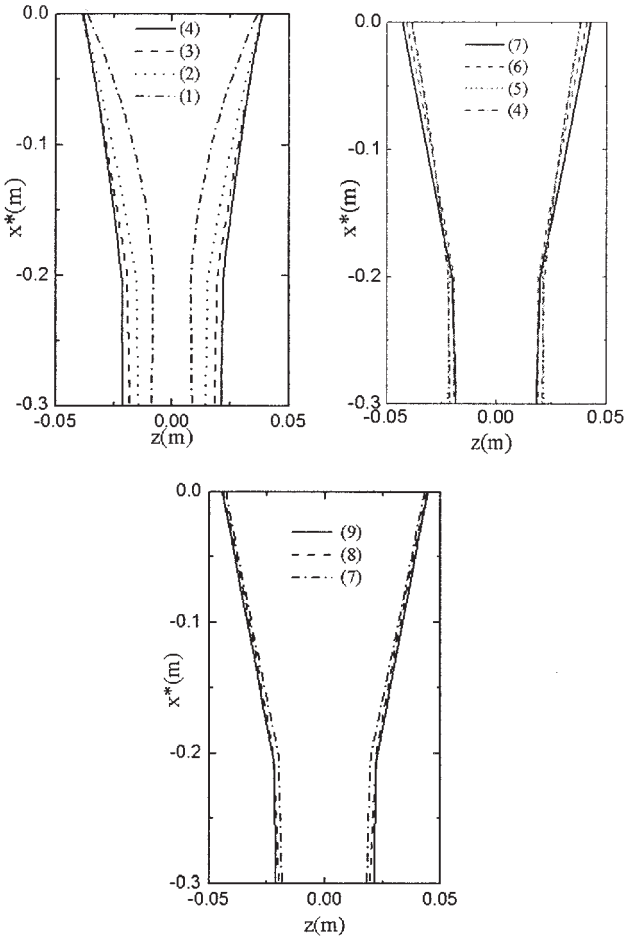

Figure 7. Shapes of heated films at different flow rates.

$T_0 = 20°C$, $T_w = 70°C$, $x^* = -x$. Units are in kg m^{-1} s^{-1}: (1) 0.03; (2) 0.06; (3) 0.09; (4) 0.12; (5) 0.15; (6) 0.18; (7) 0.24; (8) 0.30; (9) 0.36.

Results and Discussion

Calculation of the rim width

As mentioned above, D represents the width of the rim part and $(\sigma_x - \sigma_w \cos\theta)/D$ stands for the surface tension gradient in the rim. With a decrease of D, $(\sigma_x - \sigma_w \cos\theta)/D$ consequently increases and the Marangoni effect in the transverse direction of film becomes intensive. According to Figure 2, the rim part of the heated film is not flat but protuberant in the cross section. This bulgy structure is considered to result from the combination of the central film flow and the shrinkage of the film. Generally, the cross section of the rim part can be assumed to

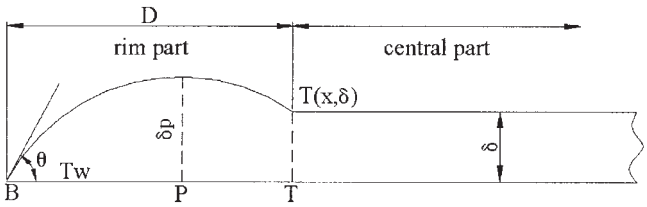

Figure 8. Cross section view of the rim part.

B, boundary of the film; P, peak of the rim; T, transitional point from the rim to central part of the film.

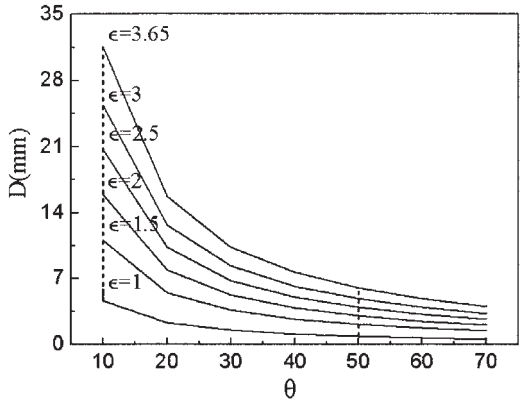

Figure 9. Variations of D with ε and θ.

be semicircular, as illustrated in Figure 8, where δ in the figure stands for the thickness of the uniform central film. δp represents the peak of bulge and θ is the contact angle of the liquid film on the plate. By using the geometrical analysis, the width of the rim part can be expressed as a function of θ, δ, and δp

$$D = \frac{\varepsilon\delta \sin\theta}{(1-\cos\theta)} + \delta\sqrt{\frac{2\varepsilon}{(1-\cos\theta)}(\varepsilon-1) - (\varepsilon-1)^2} \quad (27)$$

where

$$\delta p = \varepsilon\delta \qquad \varepsilon \geq 1 \quad (28)$$

where θ, δ, and the factor ε are, respectively, functions of physical properties of the liquid, the temperature difference between T_w and $T(x, \delta)$, and film flow rate. It is obvious that D increases with increasing film thickness δ. δ is given by Eq. 8 when the temperature is set to the average value of the inlet and outlet of the film. As an example for computing thickness of heated films at the temperature of $T_0 = 20°C$ and $T_h = 70°C$, variations of D with ε and θ at a flow rate of 0.24 kg m^{-1} s^{-1} are illustrated in Figure 9. As can be seen, D decreases noticeably with an increase of θ. In fact, the wettability of the liquid on the solid is highly related to the contact angle θ: the larger the contact angle, the less the wettability of the solid, leading to the smaller value of D. In addition, an increase of D with the factor ε can be found in Figure 9, which is clearly understand-

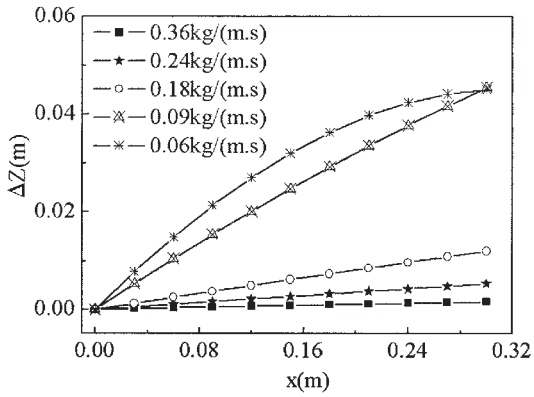

Figure 10. Variations of ΔZ vs. x.

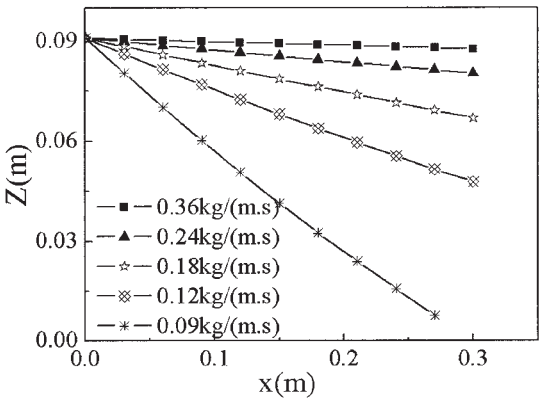

Figure 11. Variations of *Z* with *x* and liquid flow rate.

able because of the semicircular structure of the cross section of the rim in Figure 8. Moreover, D varies slightly when $\theta > 50°$ (Figure 9). $\theta = 50°$ can be regarded as the upper limit of the contact angle of the liquid on the plate, which is consistent with the fact that the receding contact angle of the distilled water on stainless steel flat plate ranges from 12 to 46°.[20] In addition, it should be noted that the width of the rim D increases along the downstream and finally reaches a maximum (Figure 1). Therefore, in the actual calculation of the shrinkage model, the average D over the contracted film was used instead of the D at a certain distance of x.

Results of calculation

The shrinkage width ΔZ of the heated film ($T_0 = 20°C$, $T_h = 70°C$) was calculated from Eq. 26. As shown in Figure 10, ΔZ increases with the increase of the distance x of film for all the liquid flow rates. ΔZ also increases with decreasing liquid flow rate at the same x. Such phenomena are in accordance with the variation of the film boundary vs. flow rate, as shown in Figure 7. Additionally, the value of ΔZ at two flow rates of 0.06 and 0.09 kg m^{-1} s^{-1} differs substantially from values at other flow rates, indicating the insufficient coverage of the film for the plate.

If Z_0 is assumed to be the initial width of the film, the width Z at distance x can be calculated as

$$Z = Z_0 - 2\Delta Z \tag{29}$$

As shown in Figure 11, Z decreases with decreasing flow rate and is dramatically reduced as the flow rate is lower than a certain value.

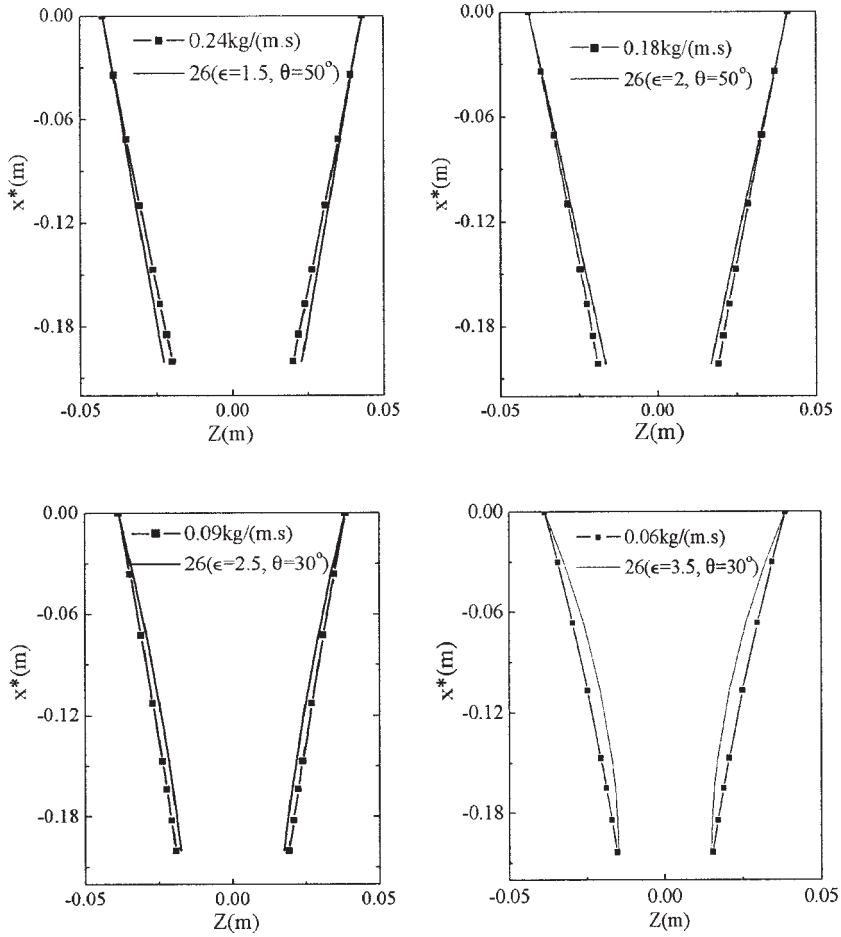

Figure 12. Comparisons of experiments with calculations.

$T_0 = 20°C$, $T_h = 70°C$.

Comparison of the model with the experiments

Comparison of the calculated results by the shrinkage model with the experimental data is made and shown in Figure 12. The symbols represent the measured film boundaries, whereas the single lines are results calculated from Eq. 26. The calculations were in good agreement with the experiments at higher flow rates of 0.24 and 0.18 kg m^{-1} s^{-1}, with deviations of 3.8 and −3.3%, respectively. With decreasing liquid flow rate, the deviations increase to −5.6 and −10.9% at flow rates of 0.09 and 0.06 kg m^{-1} s^{-1}, which are still acceptable from an industrial perspective. This implies that the model can accurately describe the shrinkage of heated falling films and thus accurately present the interfacial area. In addition, the model can be extended to a more realistic level by including the effects of evaporation at the film edge, the effect of temperature on viscosity variation, and other dynamic parameters. This will be the focus of future work.

Conclusions

The characteristics of heated falling films over a vertical stainless steel plate have been investigated both experimentally and theoretically, and the following conclusions were made:

(1) From infrared thermographic experiments of heated film flowing down a vertical stainless steel plate, it is shown that the liquid film is heated and contracted from the beginning stage of the entrance to form the shape of an inverse trapezoid. The film shrinkage and the noticeable transfer area reduction are attributed to the surface tension gradient that results from the variations of temperature in the transverse direction of the film. This indicates that the Marangoni effect arising from the existence of surface tension gradient seriously affects the falling film process.

(2) The governing equations for a laminar falling liquid film over a vertical heated plate of constant surface temperature were solved and the temperature distribution was obtained for the exact expression of Marangoni effect in the heated film.

(3) A model describing the characteristics for the shrinkage of heated falling film was established with consideration of the film flow over a vertical plate and the surface tension gradient effect in the transverse direction of the film. Comparison with the experiments demonstrated that the model could accurately describe the shrinkage characteristics of the process.

Acknowledgments

The authors are grateful for the financial support from National 985 Project of China and the National Natural Science Foundation of China (No. 20576050). We also thank Professor Youting Wu for valuable help.

Literature Cited

1. Yih SM, Seagrave RC. Hydrodynamic stability of thin liquid films flowing down an inclined plane with accompanying heat transfer and interfacial shear. *AIChE J.* 1978;24:803-810.
2. Wilson SK, Duffy BR. On the gravity-driven draining of a rivulet of fluid with temperature-dependent viscosity down a uniformly heated or cooled substrate. *J Eng Math.* 2002;42:359-372.
3. Goussis DA, Kelly RE. Effects of viscosity variation on the stability of a liquid film flow down heated or cooled inclined surfaces: Finite wavelength analysis. *Phys Fluids.* 1987;30:974-982.
4. Kabov OA, Scheid B, Sharina IA, Legros JC. Heat transfer and rivulet structures formation in a falling thin liquid film locally heated. *Int J Therm Sci.* 2002;427:664-672.
5. Ramaswamy B, Krishnamoorthy S, Joo SW. Three-dimensional simulation of instabilities and rivulet formation in heated falling films. *J Comput Phys.* 1997;131:70-88.
6. Skotheim JM, Thiele U, Scheid B. On the instability of a falling film due to localized heating. *J Fluid Mech.* 2003;475:1-19.
7. Schatz FM, Neitzel PG. Experiments on thermocapillary instabilities. *Annu Rev Fluid Mech.* 2001;33:93-127.
8. Wang KH, Ludviksson V, Lightfoot EN. Hydrodynamic stability of Marangoni films. *AIChE J.* 1971;17:1402-1408.
9. Ludviksson V, Lightfoot EN. Hydrodynamic stability of Marangoni films. *AIChE J.* 1968;14:620-626.
10. Joo SW, Davis SH, Bankoff SG. A mechanism for rivulet formation in heated falling films. *J Fluid Mech.* 1996;321:279-298.
11. Kabov OA. Breakdown of a liquid film flowing over the surface with a local heat source. *Thermophys Aeromech.* 2000;7:513-520.
12. Kabov OA, Chinnov EA. Heat transfer from a local heat source to subcooled liquid film. *High Temp.* 2001;39:703-713.
13. Zaitsev DV, Kabov OA, Evseev AR. Measurement of locally heated liquid film thickness by a double-fiber optical probe. *Exp Fluids.* 2003;34:748-754.
14. Zuber N, Staub FW. Stability of dry patches forming in liquid films flowing over heated surfaces. *Int J Heat Mass Transfer.* 1966;9:897-903.
15. Wang BX, Zhang JT, Peng XF. Experimental study on the dryout heat flux of falling liquid film. *Int J Heat Mass Transfer.* 2000;43:1897-1903.
16. Shi JS, Zhang QZ. Analysis on the breaking of subcooled falling liquid films. *Chin J Appl Mech.* 2002;19:78-80.
17. Geng J. *Influence of Marangoni Effect on Distillation in Packing Tower*. PhD Dissertation. Nanjing, China: Nanjing University; 2002.
18. Dukler AE, Bergelin OP. Characteristics of flow in falling liquid films. *Chem Eng Process.* 1952;48:557-563.
19. Saouli S, Saouli SA. Second law analysis of laminar falling film along an inclined heated plate. *Int Commun Heat Mass Transfer.* 2004;31:879-886.
20. Wang XD, Peng XF, Lu JF, Wang BX. Measuring technique of contact angle and contact angle hysteresis on rough solid surface. II: Contact angle hysteresis on rough stainless surface. *J Basic Sci Eng* (*China*). 2003;11:296-303.

Manuscript received Nov. 21, 2004, revision received Mar. 31, 2005, and final revision received Jun. 5, 2005.